

# Lifetime Measurements in $^{182,186}\text{Pt}$

J. C. Walpe,\* U. Garg, S. Naguleswaran,<sup>†</sup> and J. Wei

*Department of Physics, University of Notre Dame, Notre Dame, IN 46556*

W. Reviol

*Department of Chemistry, Washington University, St. Louis, MO 63130*

I. Ahmad, M. P. Carpenter, and T. L. Khoo

*Physics Division, Argonne National Laboratory, Argonne, IL 60439*

(Dated: November 23, 2018)

## Abstract

Lifetimes in the yrast bands of the nuclei  $^{182,186}\text{Pt}$  have been measured using the Doppler-shift Recoil Distance technique. The results in both cases *viz.* a sharp increase in  $B(E2)$  values at very low spins, may be interpreted as resulting from a mixing between two bands of different quadrupole deformations.

PACS numbers: PACS numbers: 21.10.Tg, 21.10.Ky, 27.70.+q

---

\*Present address: ADESA, Inc., Carmel, IN 46032.

<sup>†</sup>Present address: Center for Defence Communication and Information Networking, The University of Adelaide, Adelaide SA5005, Australia.

Shape-coexistence has been observed in many nuclei in the  $A \sim 180$  region [1]. For example, in the  $^{178-188}\text{Hg}$  ( $Z=80$ ) nuclei, bands of states of spin-parity  $0_1^+$ ,  $2_1^+$ ,  $4_1^+$ , ... and  $0_2^+$ ,  $2_2^+$ ,  $4_2^+$ , ..., have been observed with similar intensities [2, 3] and are known (via energy-spacing and  $B(E2)$  measurements) to have different quadrupole deformations [4, 5]; the lower-energy bands exhibit oblate shape characteristics, and the higher-energy bands exhibit prolate characteristics [6]. Indeed, all mean-field calculations [7–10] predict a coexistence of prolate and oblate shapes in this region of nuclei. There is also evidence to support shape coexistence in the light Pt ( $Z=78$ ) nuclei [11–13]. In particular, the  $B(E2)$  values in the yrast band of  $^{184}\text{Pt}$  undergo a dramatic increase in going from the  $2^+$  state to the  $6^+$  state and this increase has been interpreted as resulting from a mixing, at low spins, between two bands with deformations of different magnitude [11]. An extensive discussion of the deformation-driving aspects of all the quasiparticles, as well as shape-coexistence, in  $^{184}\text{Pt}$  has been provided in Ref.[14].

The shape-coexistence picture in the Pt nuclei has engendered extensive theoretical interest in recent years [15–19]. In particular, there has been a controversy regarding whether shape evolution in the Pt isotopes involves intruder states [17–19], or can be understood without invoking the intruder states [15, 16]. Most recently, García-Ramos *et al.* [19] have established that configuration-mixing is an essential feature of these nuclei, although it is not apparent when considering only a limited set of data; they termed this “concealed configuration mixing” and have suggested further spectroscopic measurements where this mixing might be clearly revealed. Lifetime measurements, and the extracted transition probabilities, up to the states beyond the mixing region provide such additional spectroscopic information.

In this Brief Report, we present results from lifetime measurements in the  $^{182,186}\text{Pt}$  nuclei, using the Doppler-shift recoil distance method (RDM). The primary aim of these measurements was to extend the  $^{184}\text{Pt}$  results to the nearby Pt isotopes in order to develop a better understanding of the nuclear structure properties in this transitional region. No previous lifetime information was available on the excited states in these two nuclei, save that of the first  $2^+$  state in  $^{186}\text{Pt}$ , obtained from decay of  $^{186}\text{Au}$  [20].

Two separate RDM experiments were carried out at the ATLAS facility at the Argonne National Laboratory, using the  $^{154}\text{Sm}(^{36}\text{S}, 4n)^{186}\text{Pt}$  and  $^{122}\text{Sn}(^{64}\text{Ni}, 4n)^{182}\text{Pt}$  reactions at beam energies of 167 MeV and 295 MeV, respectively. Statistical model calculations (with the code CASCADE) and brief excitation function measurements were employed to deter-

mine the beam energies for the optimal population of the  $4n$  channels. In the case of  $^{186}\text{Pt}$ , the target was enriched  $^{154}\text{Sm}$  evaporated, to a thickness of  $500 \mu\text{g}/\text{cm}^2$ , onto a stretched  $1.2 \text{ mg}/\text{cm}^2$ -thick Au foil. For the  $^{182}\text{Pt}$  experiment, the target used was similarly prepared with enriched  $^{122}\text{Sn}$  evaporated onto a  $1.5 \text{ mg}/\text{cm}^2$ -thick Au foil to a thickness of  $850 \mu\text{g}/\text{cm}^2$ . The targets were mounted in the Notre Dame “plunger” device, with the Au surface facing the beam. The plunger device consisted of three dc actuators which are used for precision placement of the target foil with respect to a fixed stopper foil (a stretched, self-supporting, Au foil of  $10.0 \text{ mg}/\text{cm}^2$  thickness in the case of  $^{186}\text{Pt}$  and  $25 \text{ mg}/\text{cm}^2$  thickness in the case of  $^{182}\text{Pt}$ ). Gamma-ray spectra were recorded using the Argonne-Notre Dame  $\gamma$ -ray Facility, which consisted of twelve Compton-suppressed HPGe detectors and a 50-element BGO multiplicity array. Four detectors each were placed at angles of  $34^\circ$  (“forward-angle”),  $90^\circ$ , and  $146^\circ$  (“backward-angle”) with respect to the beam direction. Data were collected for approximately 3 hours at each of 18 and 24 target-to-stopper distances for  $^{186}\text{Pt}$  and  $^{182}\text{Pt}$ , respectively, ranging from the closest attainable distances (corresponding to electrical contact) of  $15 \mu\text{m}$  ( $^{186}\text{Pt}$ ) and  $9 \mu\text{m}$  ( $^{182}\text{Pt}$ ) to a maximum distance of  $\sim 10000 \mu\text{m}$  in each case. This resulted in an effective measurable lifetime range of  $\sim 2 \text{ ps}$  to  $\geq 1 \text{ ns}$ .

Sample spectra for several recoil distances, taken with the detectors placed at  $34^\circ$ , are shown in Fig. 1 and Fig. 2, with the corresponding recoil distance given in the upper right corner of each spectrum. The level schemes of these nuclei are known from Refs.[21, 22] and the transitions of interest are labelled. Lifetime information was reliably extracted for yrast transitions up to the  $16^+$  ( $14^+$ ) level in  $^{186}\text{Pt}$  ( $^{182}\text{Pt}$ ). For each transition, a set of ratios,  $R_d$ , defined as the ratio of the intensity of the unshifted  $\gamma$ -ray peak to the total intensity of the unshifted and the associated shifted peak at recoil distance  $d$ , were determined. Each set of  $R_d$  values defined a decay curve for a given transition. All such  $R_d$  curves were fitted simultaneously with a combination of exponential functions and the lifetime for each level was extracted from these fits. The computer code LIFETIME [23] was employed in the fitting procedure. This code allows for all the “standard” corrections to be applied to the data: changes in the solid angle subtended by the detectors due to the changing ion position along the flight path; changes in solid angle subtended by the detector due to the relativistic motion of the ion; changes in the angular distribution due to the attenuation of alignment while the ion was in flight; and, slowing of the ion in the stopper material. In addition, corrections were made to the data to account for the detector efficiencies and

internal conversion. A crucial aspect of data analysis was accounting for the effects of cascade feeding, both observed and unobserved, from higher-lying states. A two-path feeding process into the level was assumed for each instance where the observed intensity feeding into the level was less than the observed intensity decaying out of it. One of the feedings is from the next highest transition in the yrast cascade, which represents the cumulative effect of the decay of all higher members of the cascade, while the other represents all unobserved feeding, *i.e.*, feeding from the  $\gamma$ -ray continuum and non-yrast states. The relative intensities for the observed states were determined from the data collected by the detectors placed at  $90^\circ$ . Initial relative intensities for the levels representing the unobserved feeding were determined by taking the difference between the observed intensity into a given level and the observed intensity out of the said level.

The resulting fits to the experimental data are presented in Fig. 3 and the extracted lifetimes as well as the corresponding B(E2) values are given in Tables I and II; preliminary results have been reported previously [24, 25]. We note that the lifetime obtained for the  $2^+$  state in  $^{186}\text{Pt}$  is consistent with the “adopted value” in the compilation by Raman *et al.* [20, 26]. Further, of all the theoretical predictions listed in Ref.[26], the B(E2)’s for the  $2^+$  states in  $^{182,184,186}\text{Pt}$  obtained in our measurements are closest to those from the Woods-Saxon Model (WSM in Ref.[26]).

As can be seen in the Tables and Fig. 4, there is indeed a sharp increase in the B(E2) value when going from the  $2^+$  to the  $6^+$  state in each case, similar to the observation in  $^{184}\text{Pt}$  [11]. In a deformed rotor interpretation, this change in B(E2) value corresponds to an increase in deformation from  $\beta_2=0.20$  for the  $2^+$  state to  $\beta_2=0.25$  for the  $6^+$  state in  $^{186}\text{Pt}$  and from  $\beta_2=0.19$  for the  $2^+$  state to  $\beta_2=0.25$  for the  $6^+$  state in  $^{182}\text{Pt}$ . [If this were an undisturbed rotational band, the  $\beta_2$  value would be nearly a constant.]. These results are in qualitative agreement with the calculations presented in Ref.[14].

A likely explanation for this increase in the associated deformation is that there is a mixing of states at low spins. Dracoulis *et al.* [12, 13] had interpreted such increase in the deformation in the Pt nuclei as resulting from a mixing of coexisting bands and, in performing two-band mixing calculations in  $^{176-178}\text{Pt}$ , obtained results consistent with the observed behavior of the bandhead energies and mixing matrix elements. We have performed similar band-mixing calculations for the nuclei studied here, the results of which are shown in Fig. 4; the results from  $^{184}\text{Pt}$  [11] are also included for comparison. It has been assumed

in these calculations that the bands mix at low spins only, and that the  $8^+$  level in both cases is completely unmixed. The unperturbed energies of the yrast bands (called B1) were then calculated using a rotational constant of  $\hbar^2/2\mathcal{J} = 15.51$  (14.36) keV for  $^{186}\text{Pt}$  ( $^{182}\text{Pt}$ ), obtained from the respective  $8^+ \rightarrow 6^+$  transition energies. The mixing bands (called B2) were assumed to be built on the low-lying  $0_2^+$  states, at 472 (500) keV in  $^{186}\text{Pt}$  ( $^{182}\text{Pt}$ ) [27]. Calculations for the mixing between the  $0_1^+$  state (in B1) and the  $0_2^+$  state (in B2) resulted in interactions,  $V_{int}$ , between the unmixed states of 259 (237) keV for  $^{186}\text{Pt}$  ( $^{182}\text{Pt}$ ). These mixing interactions are comparable to those obtained in two-band model calculations by Thiamová and Van Isacker [28]. The calculations also imply that the ground-state band in  $^{186}\text{Pt}$  is composed of 56% B1 (larger deformation) and 44% B2 (smaller deformation), whereas the ground-state band in  $^{182}\text{Pt}$  is composed of 66% B1 and 34% B2. These results are very similar to those obtained in Ref. [11] for  $^{184}\text{Pt}$  and are consistent with the theoretical results in Refs. [18, 19], supporting a band-mixing interpretation of this B(E2) increase at low spins in these nuclei.

The results presented in Fig. 4 also exhibit a steep decline in B(E2) values beyond the  $10^+$  state in both nuclei. Some of this decline comes naturally because of the alignment of the  $i_{13/2}$  neutrons that is associated with a loss of collectivity in a limited spin range. In many transitional nuclei, a similar decline in B(E2)'s has been attributed to the possible onset of triaxiality, with positive values of  $\gamma$ , the classic example being that of the Yb nuclei [29]. This reduction in B(E2)'s (and, hence, in  $Q_t$ ) is also consistent with the theoretical results presented in Ref. [9].

Very recently, results of another lifetime measurement on  $^{182}\text{Pt}$  have become available [30]. In that work, lifetimes have been measured up to the  $10^+$  state and their results are in good agreement with those presented here, albeit the quoted uncertainties in Ref. [30] are larger. They also have presented calculations within the Interacting Boson Model and the General Collective Model, both of which indicate shape coexistence in this nucleus, in general agreement with the conclusions presented here.

In summary, we have measured the lifetimes of the yrast states in  $^{182}\text{Pt}$  and  $^{186}\text{Pt}$  up to spins  $14^+$  and  $16^+$ , respectively, using the Doppler-shift recoil distance technique. A sharp increase in the B(E2) value in going from the  $2^+$  state to the  $6^+$  state is observed in both nuclei. This increase can be understood, in the traditional way, in terms of the mixing of coexisting bands of different deformations at low spins and two-band mixing calculations are

in good agreement with the observed experimental results. We wish to emphasize, however, that the two-band mixing interpretation of these data might not be unique. Indeed, it would appear that the observed  $B(E2)$ 's in  $^{182}\text{Pt}$  can be reproduced reasonably well in IBA-1 calculations using the parameters provided in Ref. [16]. Further measurements, especially of lifetimes of non-yrast states, could be very useful in unambiguously deciding between the competing theoretical approaches to understanding the nuclear structure in this region.

We wish to acknowledge K.B. Beard (Notre Dame), I. Bearden (Purdue Univ.), R.V.F. Janssens (Argonne), S. Shastry (SUNY, Plattsburgh), and D. Ye (Notre Dame) for their important contributions to these measurements. This work has been supported in part by the National Science Foundation (Grant No. PHY-1068192) and the U.S. Department of Energy, Nuclear Physics Division, under contract no. DE-AC02-06CH11357.

- 
- [1] Kris Heyde and John L. Wood, *Rev Mod. Phys.* **83**, 1467 (2011).
  - [2] J.H. Hamilton, P.G. Hansen, and E.F. Zganjar, *Rep. Prog Phys.* **48**, 631 (1985).
  - [3] M.P. Carpenter *et al.*, *Phys. Rev. Lett.* **78**, 3650 (1997).
  - [4] J.D. Cole *et al.*, *Phys. Rev. C* **30**, 1267 (1984).
  - [5] R. Beraud *et al.*, *Nucl. Phys.* **A284**, 221 (1977).
  - [6] R. Bengtsson, T. Bengtsson, J. Dudek, G. Leander, W. Nazarewicz, and J.-Y. Zhang, *Phys. Lett.* **B183**, 1 (1987).
  - [7] S. Aberg, H. Flocard, and W. Nazarewicz, *Annu. Rev. Nucl. Part. Sci.* **40**, 439 (1990).
  - [8] P. Sarriguren *et al.*, *Phys. Rev. C* **77**, 064322 (2008).
  - [9] R. Rodríguez-Guzmán *et al.*, *Phys. Rev. C* **81**, 024310 (2010).
  - [10] K. Nomura *et al.*, *Phys. Rev. C* **83**, 014309 (2011).
  - [11] U. Garg *et al.*, *Phys. Lett.* **B180**, 319 (1986).
  - [12] G. Dracoulis, A.E. Stuchbery, A.P. Byrne, A.R. Poletti, S.J. Poletti, J. Gerl, and R.A. Bark, *J. Phys. G* **12**, L97 (1986).
  - [13] G.D. Dracoulis, *Phys. Rev. C* **49**, 3324 (1994).
  - [14] M.P. Carpenter *et al.*, *Nucl. Phys.* **A513**, 125 (1990).
  - [15] E.A. McCutchan, R.F. Casten, and N.V. Zamfir, *Phys. Rev. C* **71**, 061301(R) (2005).
  - [16] E.A. McCutchan, and N.V. Zamfir, *Phys. Rev. C* **71**, 054306 (2005).

- [17] Irving O. Morales *et al.*, Phys. Rev. C **78**, 024303 (2008).
- [18] J.E. García-Ramos and K. Heyde, Nucl. Phys. **A825**, 39 (2009).
- [19] J.E. García-Ramos, V. Hellemans, and K. Heyde, Phys. Rev. C **84**, 014331 (2011).
- [20] M. Finger *et al.*, Nucl. Phys. **A188**, 369 (1972).
- [21] D.G. Popescu *et al.*, Phys. Rev. C **55**, 1175 (1997).
- [22] C.M. Baglin, Nucl. Data Sheets **82**, 1 (1997).
- [23] Program LIFETIME, obtained from Prof. J.C. Wells, Tennessee Technological University, Cookeville, TN.
- [24] J. Wei *et al.*, Bull. Am. Phys. Soc. **35**, 1016 H6 7 (1990).
- [25] J.C. Walpe *et al.*, Bull. Am. Phys. Soc. **39**, 1419 DD4 (1994).
- [26] S. Raman, C.W. Nestor, Jr., and P. Tikkanen, At. Data Nuc. Data Tables **78**, 1 (2001).
- [27] G. Hebbinghaus *et al.*, Z. Phys. **A328**, 387 (1987).
- [28] G. Thiamová and P. Van Isacker, Phys. Scr. **64**, 23 (2001).
- [29] N.R. Johnson, Prog. Part. Nuc. Phys. **28**, 215 (1992).
- [30] K.A. Gladinski *et al.*, Nucl. Phys. **A877**, 19 (2012).

TABLE I: Lifetimes, associated B(E2) values, and the extracted transition quadrupole moments,  $Q_t$ , for  $^{186}\text{Pt}$

$E_\gamma(\text{keV})$	$I_i \rightarrow I_f$	$\tau(\text{ps})$	$B(\text{E}2)\downarrow(\text{e}^2b^2)$	$Q_t (eb)$
191.4	$2^+ \rightarrow 0^+$	$318\pm 24$	$0.69\pm 0.05$	$5.87\pm 0.22$
298.8	$4^+ \rightarrow 2^+$	$27.3\pm 1.9$	$1.15\pm 0.08$	$6.37\pm 0.22$
387.2	$6^+ \rightarrow 4^+$	$5.1\pm 0.4$	$1.77\pm 0.14$	$7.53\pm 0.30$
465.4	$8^+ \rightarrow 6^+$	$2.0\pm 0.2$	$1.80\pm 0.18$	$7.42\pm 0.37$
515.4	$10^+ \rightarrow 8^+$	$1.2\pm 0.1$	$1.86\pm 0.16$	$7.43\pm 0.31$
478.8	$12^+ \rightarrow 10^+$	$2.0\pm 0.2$	$1.56\pm 0.16$	$6.76\pm 0.34$
489.2	$14^+ \rightarrow 12^+$	$2.1\pm 0.2$	$1.38\pm 0.13$	$6.30\pm 0.30$
571.1	$16^+ \rightarrow 14^+$	$1.1\pm 0.2$	$1.23\pm 0.22$	$5.93\pm 0.54$
658.0	$18^+ \rightarrow 16^+$	$1.6\pm 0.2^a$		

TABLE II: Lifetimes, associated B(E2) values, and the extracted transition quadrupole moments,  $Q_t$ , for  $^{182}\text{Pt}$

$E_\gamma(\text{keV})$	$I_i \rightarrow I_f$	$\tau(\text{ps})$	$B(\text{E}2)\downarrow(\text{e}^2b^2)$	$Q_t (eb)$
155.0	$2^+ \rightarrow 0^+$	$709\pm 43$	$0.66\pm 0.04$	$5.77\pm 0.17$
264.3	$4^+ \rightarrow 2^+$	$47.5\pm 2.9$	$1.15\pm 0.07$	$6.37\pm 0.19$
355.0	$6^+ \rightarrow 4^+$	$7.8\pm 0.5$	$1.74\pm 0.11$	$7.45\pm 0.24$
430.9	$8^+ \rightarrow 6^+$	$3.4\pm 0.3$	$1.55\pm 0.12$	$6.88\pm 0.27$
492.6	$10^+ \rightarrow 8^+$	$1.7\pm 0.2$	$1.63\pm 0.13$	$6.95\pm 0.28$
543.5	$12^+ \rightarrow 10^+$	$1.7\pm 0.1$	$0.97\pm 0.11$	$5.33\pm 0.30$
590.0	$14^+ \rightarrow 12^+$	$1.6\pm 0.2$	$0.69\pm 0.07$	$4.47\pm 0.23$
628.5	$16^+ \rightarrow 14^+$	$3.3\pm 0.4^a$		

<sup>a</sup>Lifetimes of the  $18^+$  and  $16^+$  levels, respectively, could not be separated from the side feeding lifetimes.

The values given are therefore upper limits.



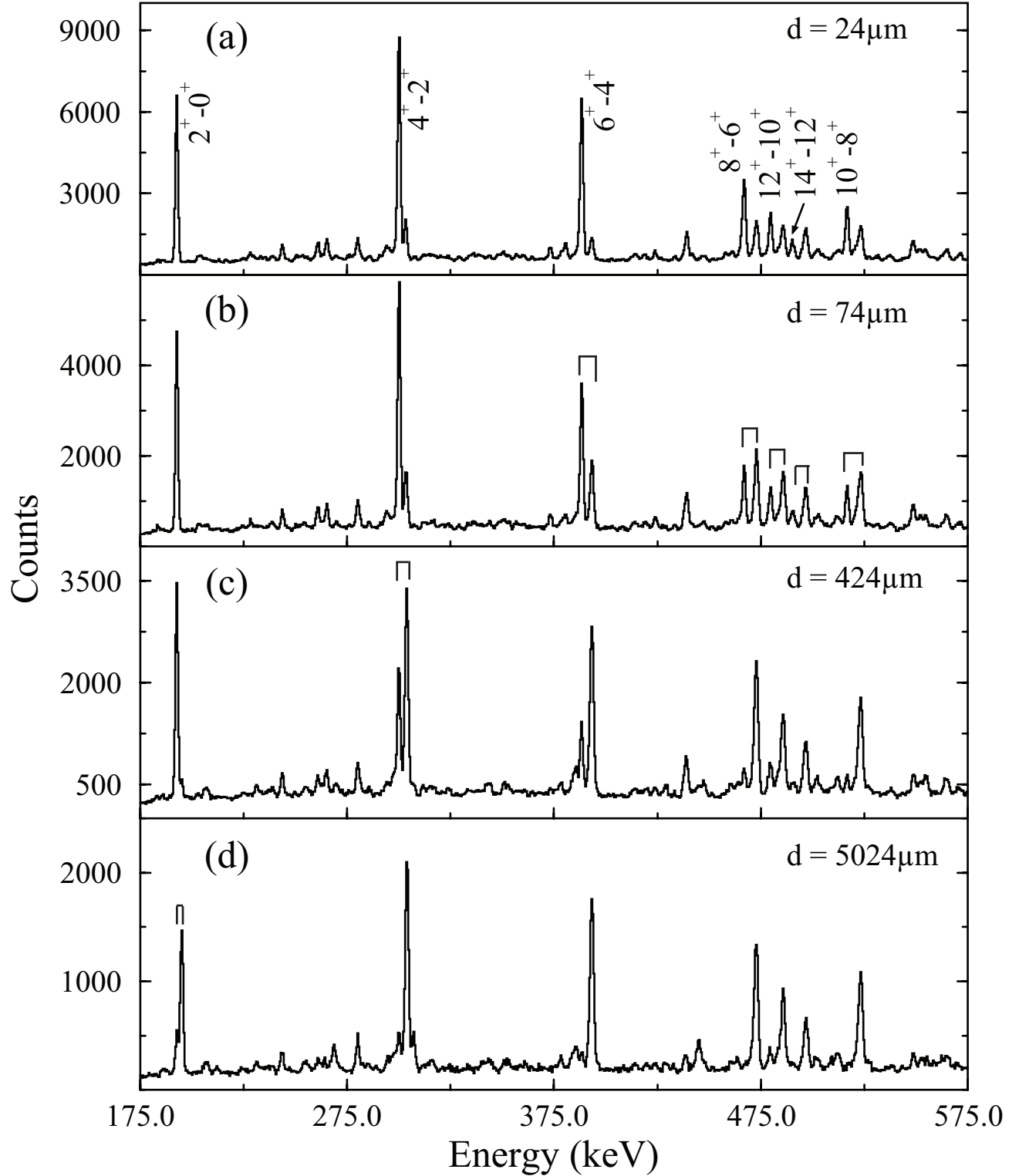


FIG. 1: Sample spectra from the “forward-angle” detectors for  $^{186}\text{Pt}$  at the indicated recoil distances. The transitions of interest are marked. The relative increase in the intensities of the “shifted” peaks with increasing distance is clearly visible.

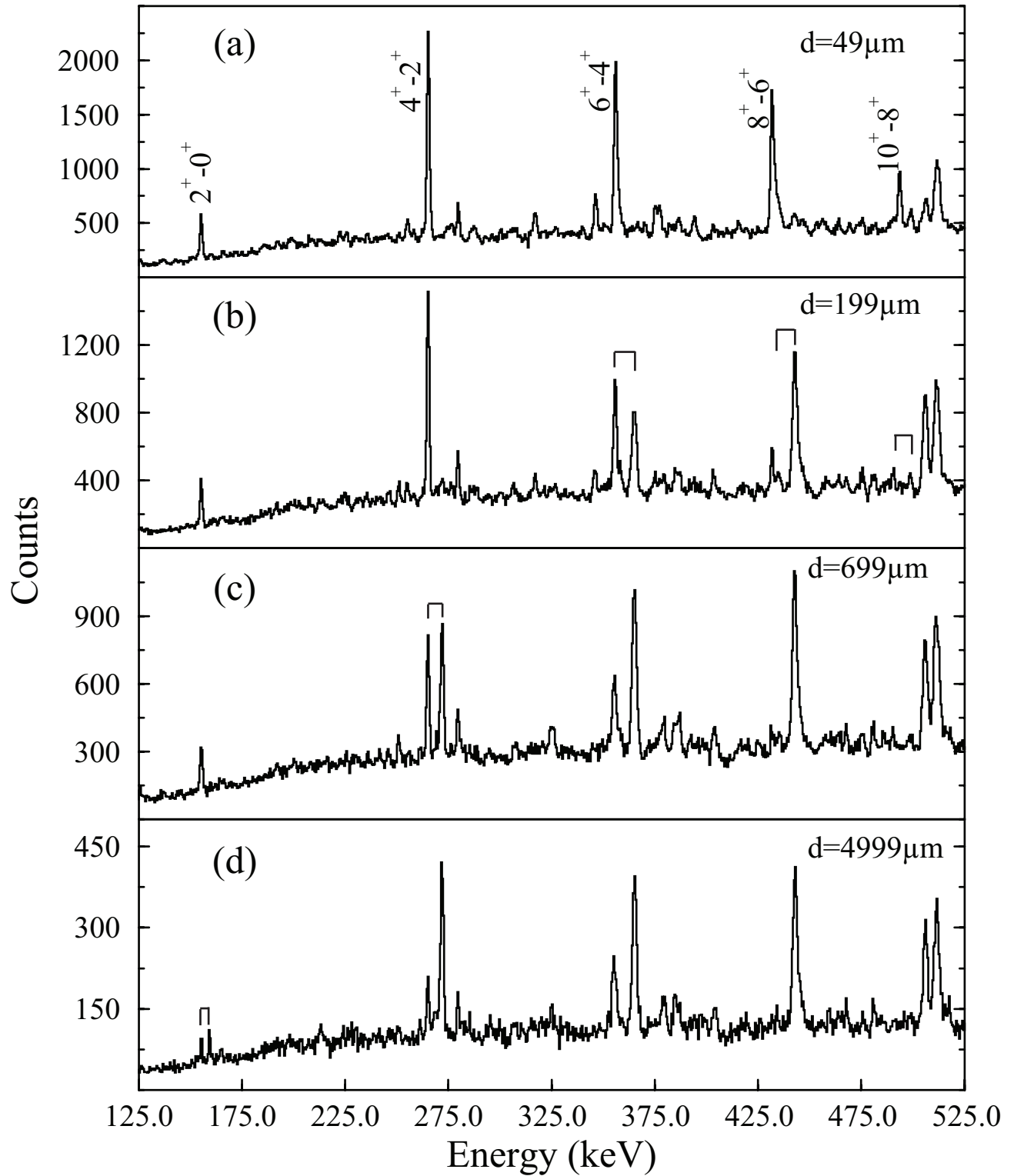


FIG. 2: Same as Fig. 1, but for  $^{182}\text{Pt}$ .

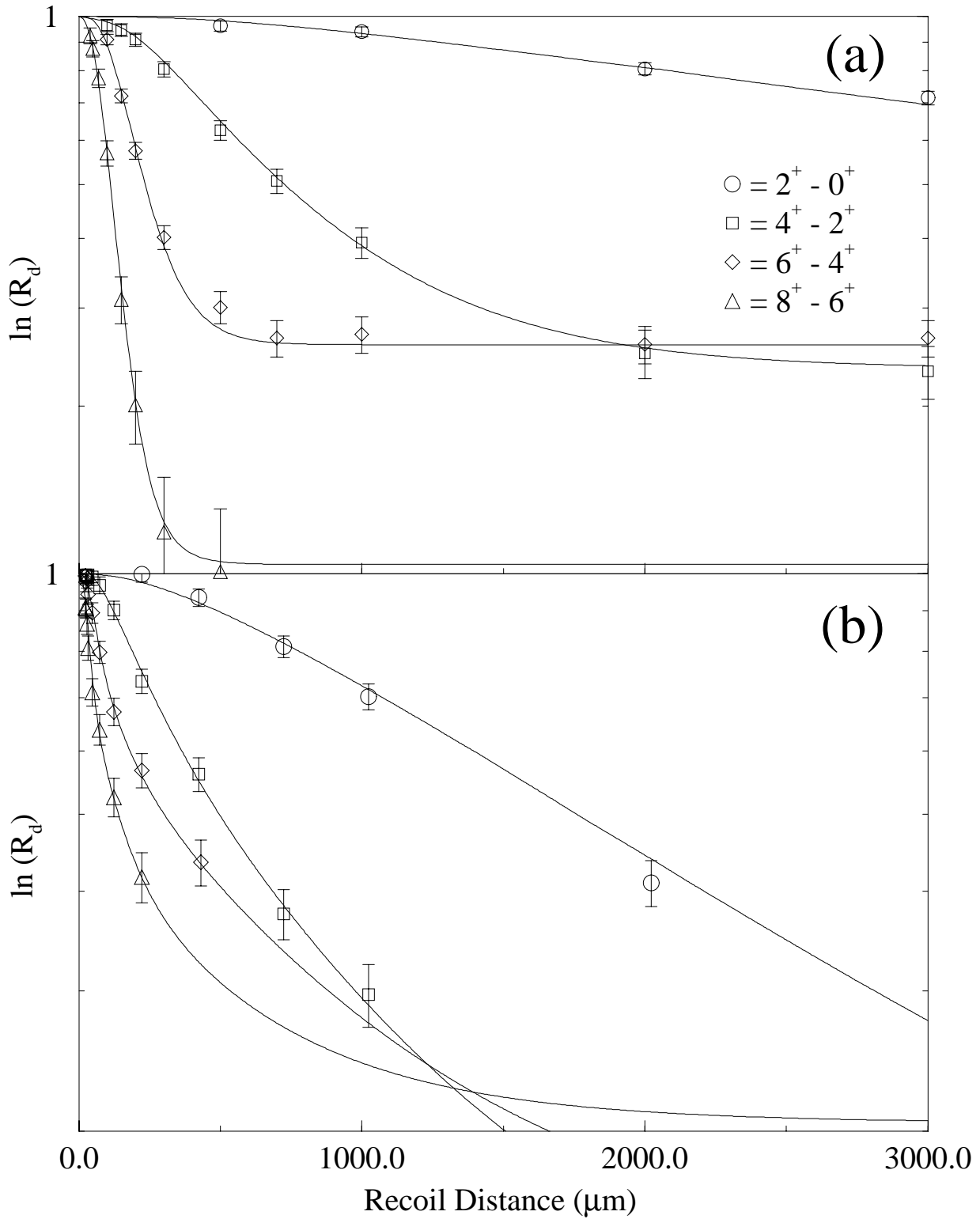


FIG. 3: Fits to the ratios  $R_d$  as a function of the recoil distance for the lowest yrast transitions in (a)  $^{186}\text{Pt}$  and (b)  $^{182}\text{Pt}$ , as obtained from the code LIFETIME.

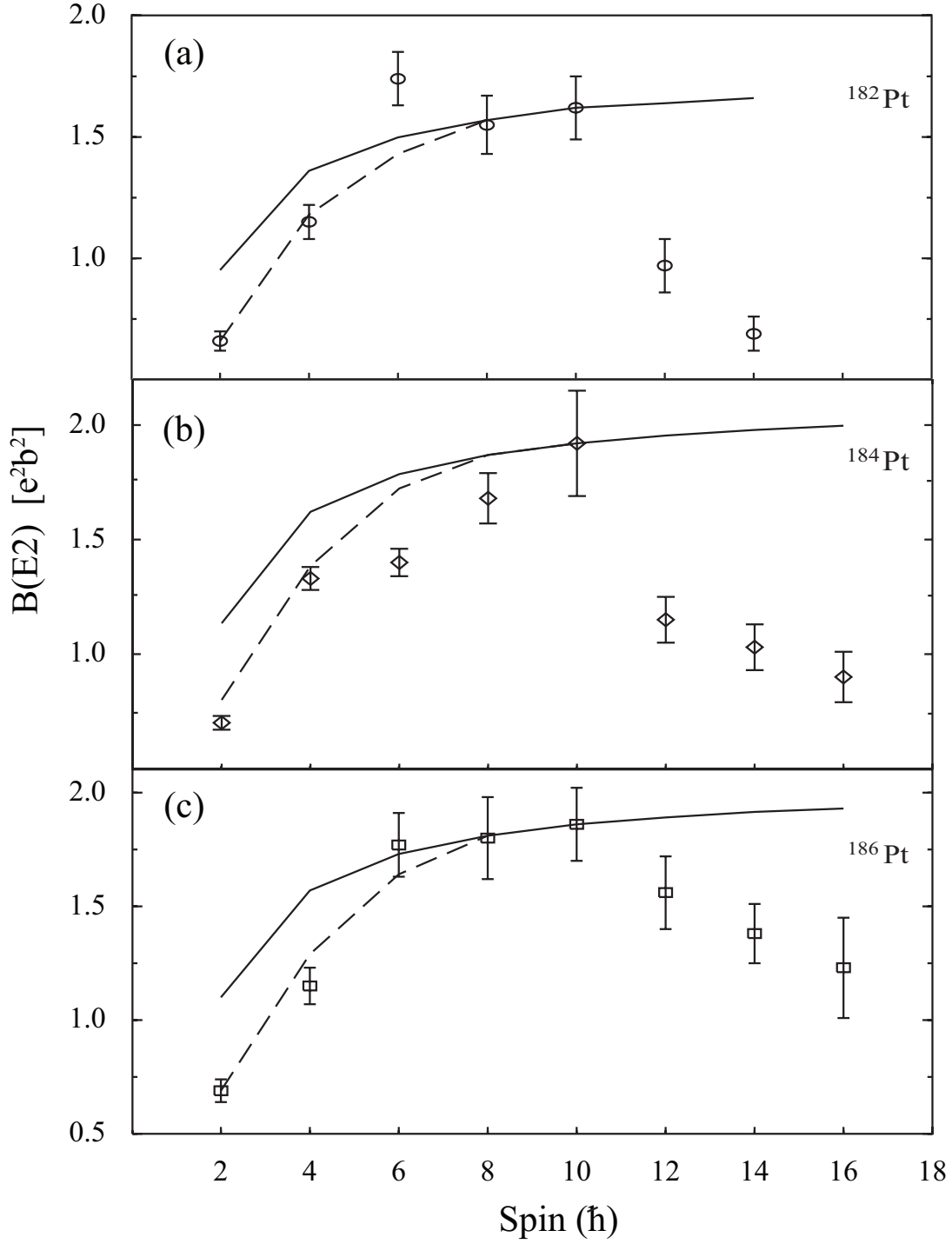


FIG. 4:  $B(E2)$  vs. the spin of the depopulating state for  $^{182}\text{Pt}$  (panel (a)) and  $^{186}\text{Pt}$  (panel (c)). The experimental results from the present work are shown, along with the expected results for a rigid rotor with deformation corresponding to the  $10^+ \rightarrow 8^+$  transition (solid lines) and the results of two-band mixing calculations (dashed lines; see text). The results for  $^{184}\text{Pt}$  (taken from Ref. [11]) are also shown (panel (b)) for comparison.